

Jets in Heavy Ion Collisions with the ATLAS Detector

Helena Santos (on behalf of the ATLAS Collaboration)

LIP - Laboratório de Instrumentação e Física Experimental de Partículas, Portugal

Published 3 May 2018

Jets constitute a golden probe to study the quark gluon plasma produced in heavy ion collisions at the LHC. Being produced at the early stages of the collisions, they are expected to be modified as propagating through the hot and dense medium. A signature of the modification is the energy loss lowering the jet yields at a given transverse momentum. A factor of two suppression is observed in central Pb+Pb collisions with respect to pp collisions. Other signatures are the modification of the dijet momentum balance and the modification of fragmentation functions. These proceedings describe results on these observables from ATLAS in Runs 1 and 2. The high statistical significance of these data samples collected by ATLAS allows precision measurements of these observables in a wide range of transverse momentum and centrality.

Keywords: Quark Gluon Plasma; Jet Quenching; Fragmentation Functions; Dijet asymmetry.

1. Introduction

A wide research program is ongoing at the Large Hadron Collider with the aim of studying the properties of QCD matter at extreme temperatures and densities. Jets produced in ultra-relativistic heavy ion collisions constitute a golden probe of such a state of matter. The hard scattered quarks and gluons emerged from these collisions evolve as parton showers that propagate through the hot and dense medium. Constituents of the parton showers emit medium-induced gluon radiation and, as a consequence, the resulting jet loses energy, a phenomenon commonly termed as jet quenching¹. Jets produced in heavy ion collisions are thus expected to be suppressed at a given p_T , relatively to a sample produced in pp collisions. Their internal structure is also expected to be modified. The large acceptance and high granularity of the ATLAS detector² is well suited to study these phenomena. Results shown in this conference use data produced in Pb+Pb, p +Pb, and pp collisions at the center of mass energies of 2.76 TeV and 5.02 TeV. The centrality of the

This is an Open Access article published by World Scientific Publishing Company. It is distributed under the terms of the Creative Commons Attribution 4.0 (CC-BY) License. Further distribution of this work is permitted, provided the original work is properly cited.

Pb+Pb collisions is estimated using the total transverse energy deposited in the forward calorimeters ($\sum E_T^{\text{FCal}}, 3.2 \leq |\eta| < 4.9$) and compared to a Glauber Monte Carlo model³, convoluted with pp data taken at the same beam energy. The $\sum E_T^{\text{FCal}}$ distribution is then divided into percentiles of the total inelastic cross-section for Pb+Pb collisions. Jets are reconstructed using calorimeter “towers” as input signals to the anti- k_t algorithm, with jet radius parameter size $R = 0.4$. The underlying event is estimated and subtracted event-by-event in each calorimeter layer and strip of pseudorapidity after excluding regions subtending jet candidates and corrected for flow modulation.

2. Results

The nuclear modification factor R_{AA} , defined as the ratio of normalized yields in Pb+Pb and pp collision systems, is used to compare the inclusive transverse momentum distributions measured in the two collision systems:

$$R_{AA} \equiv \frac{(1/N_{\text{evt}}) \, d^2 N_{\text{jet}}^{\text{PbPb}}/dp_T dy|_{\text{cent}}}{\langle T_{AA} \rangle \, d^2 \sigma_{\text{jet}}^{\text{pp}}/dp_T dy}, \quad (1)$$

where $\langle T_{AA} \rangle$ stands for the geometric enhancement of per-collision nucleon-nucleon luminosity and N_{evt} is the total number of Pb+Pb collisions within a chosen centrality interval. The measurement of R_{AA} , unfolded for detector resolution, bin-to-bin migration and reconstruction inefficiency, is shown in Fig.1. Jets are suppressed increasingly with collision centrality, reaching a factor of two in central collisions (0–10%), while showing little dependence on jet transverse momentum⁴. These measurements confirm the expectations on the reduction of the jet yields at a given transverse momentum due to the interaction of partons in the quark gluon plasma¹.

Jet fragmentation functions are measured aiming a deeper understanding of the jet energy loss nature and constraining jet quenching models. The jet structure is probed in the p_T range from 126 to 398 GeV, using tracks with $p_T^{\text{ch}} > 4$ GeV and $p_T^{\text{ch}} > 1$ GeV in Pb+Pb collisions at the nucleon-nucleon center of mass energy $\sqrt{s_{\text{NN}}}=5.02$ TeV and 2.76 TeV, respectively. The fragmentation functions, defined as $D[z(p_T)] = (1/N_{\text{jet}}) dN_{\text{ch}}/dz(p_T)$, where N_{jet} and N_{ch} stand for the number of jets and charged particles, respectively, are studied as a function of the longitudinal momentum fraction, $z = p_T^{\text{ch}}/p_T^{\text{jet}} \cos \Delta R$. The measured $D(z)$ are background subtracted, corrected for reconstruction inefficiency and unfolded with a 2D Bayesian method. The left panel of Fig. 2 shows the modification of the fragmentation functions, assessed with $R_{D(z)} = D(z)|_{\text{Pb+Pb}}/D(z)|_{\text{pp}}$, in central collisions (0–10%) for the two center of mass energies, $\sqrt{s_{\text{NN}}}=5.02$ TeV and 2.76 TeV. The larger phase space of the measurement at $\sqrt{s_{\text{NN}}}=2.76$ TeV allows the observation of an enhancement at low z , up to 0.03. In the intermediate range of $0.03 < z < 0.2$ both distributions show a depletion followed by an enhancement up to $z = 1$, suggesting that the modification of the fragmentation functions does not depend on the center of mass energy. The enhancement of fragment yields at low z is consistent with an interpretation in which the energy lost by partons is transferred

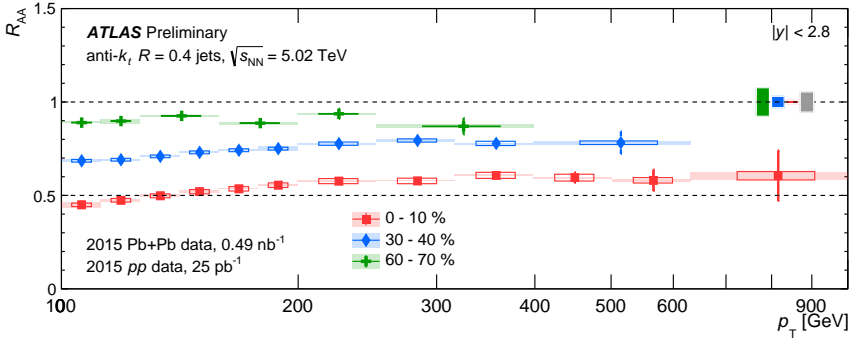


Fig. 1. The R_{AA} as a function of jet p_T for jets with $|y| < 2.8$ for three centrality bins. The error bars represent statistical uncertainties, the shaded boxes around the data points represent correlated systematic uncertainties, open boxes represent uncorrelated systematic uncertainties. The colored shaded boxes at unity represent $\langle T_{AA} \rangle$ uncertainties and the gray shaded box represents the uncertainty on pp luminosity. The horizontal width on the shaded boxes represents the width of the p_T interval and the horizontal widths on the open boxes are arbitrary for better visibility⁴.

predominantly to soft particles⁶. The right panel shows $R_{D(z)}$ for different ranges of the transverse momentum of the jet. No dependence with this variable is verified. Details on this analysis can be found in Ref. 7. Jet fragmentation functions have also been studied in proton-lead collisions at $\sqrt{s_{NN}}=5.02$ TeV⁸. The measured $R_{D(z)} = D(z)|_{p+Pb}/D(z)|_{pp}$, integrated in collision centrality (0–90%), is consistent with unity independently of the jet p_T range, as can be seen in Fig. 3.

The first indication of jet quenching was given by the observation of large asymmetric dijet events⁹. Dijets probe differences in the two parton showers since in most of the cases the interaction of the two outgoing partons in the quark gluon plasma is not identical. A new analysis has been performed using $140 \mu b^{-1}$ of Pb+Pb data taken at $\sqrt{s_{NN}}=2.76$ TeV and benefiting from a deeper understanding of the underlying event and analysis conditions. Figure 4 shows the distribution of dijets produced in Pb+Pb and pp collisions as a function of x_J , the ratio between the transverse momenta of the two leading jets. The measured distributions are unfolded to account for the effects of experimental resolution and inefficiencies on the two-dimensional (p_{T1}, p_{T2}) distributions and then projected into bins of fixed ratio $x_J = p_{T1}/p_{T2}$. The observation of large asymmetric dijets in central collisions is striking. The distributions in the two colliding systems become increasingly similar with decreasing centrality. Particularly interesting is the study of the variation of the dijet asymmetry with the p_T of the leading jet. A modification in the asymmetry in Pb+Pb collisions as the p_T of the leading jet increases is observed, indicating that higher transverse momentum jets lose less energy relatively to the leading jet and so tend to be more balanced. This feature is particularly evident for transverse momentum greater than 200 GeV. Details on this analysis can be found in Ref. 10.

The study of photon-jet asymmetry is particularly important because photons do not interact with the QCD medium. Any observed asymmetry is entirely

H. Santos

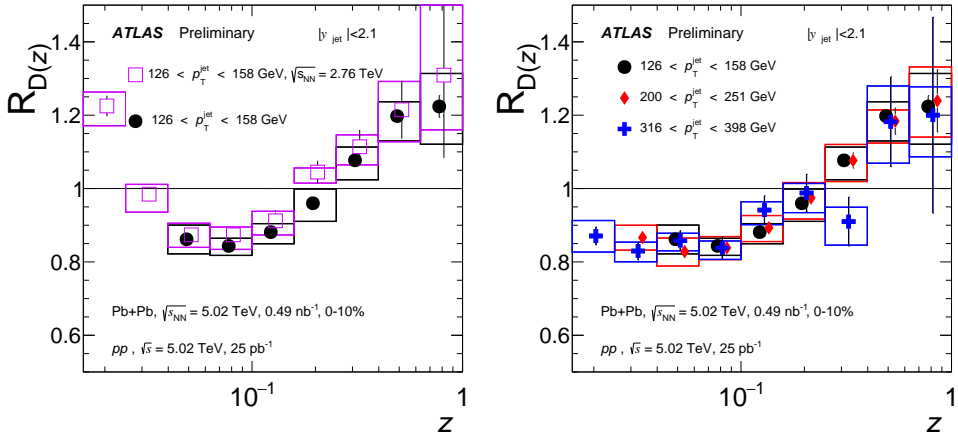


Fig. 2. Left: $R_{D(z)}$ measured at $\sqrt{s_{NN}} = 5.02$ TeV collisions (black circles) and at 2.76 TeV (open squares) for the p_T^{Jet} jet interval from 126-158 GeV. Right: The same quantity as in the left panel for three p_T^{Jet} selections: 126-158 GeV (black circles), 200-251 GeV (red diamonds) and 316-398 GeV (blue crosses). The statistical uncertainties are shown as bars and the systematic uncertainties as outlined boxes⁷.

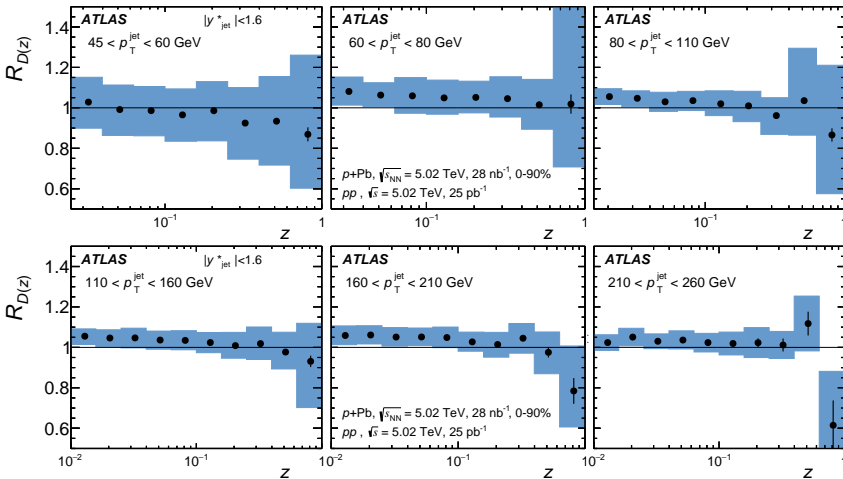


Fig. 3. $R_{D(z)}$ in $p+Pb$ collisions to those in pp collisions for the six p_T^{Jet} intervals. The statistical uncertainties are shown as error bars and the total systematic uncertainties are shown as shaded boxes⁸.

due to jet energy loss and the photon constitutes a precious calibration probe. In the current analysis the transverse momentum and rapidity of the jet is, respectively, $p_T^{Jet} > 30$ GeV and $|y^{Jet}| < 2.1$. The jet is required to be nearly in the opposite direction of the photon ($\Delta\phi_{J\gamma} > 7\pi/8$)¹¹. Figure 5 shows that the photon-jet $x_{J\gamma} = p_T^{Jet}/p_T^\gamma$ is increasingly modified with increasing centrality, relative to

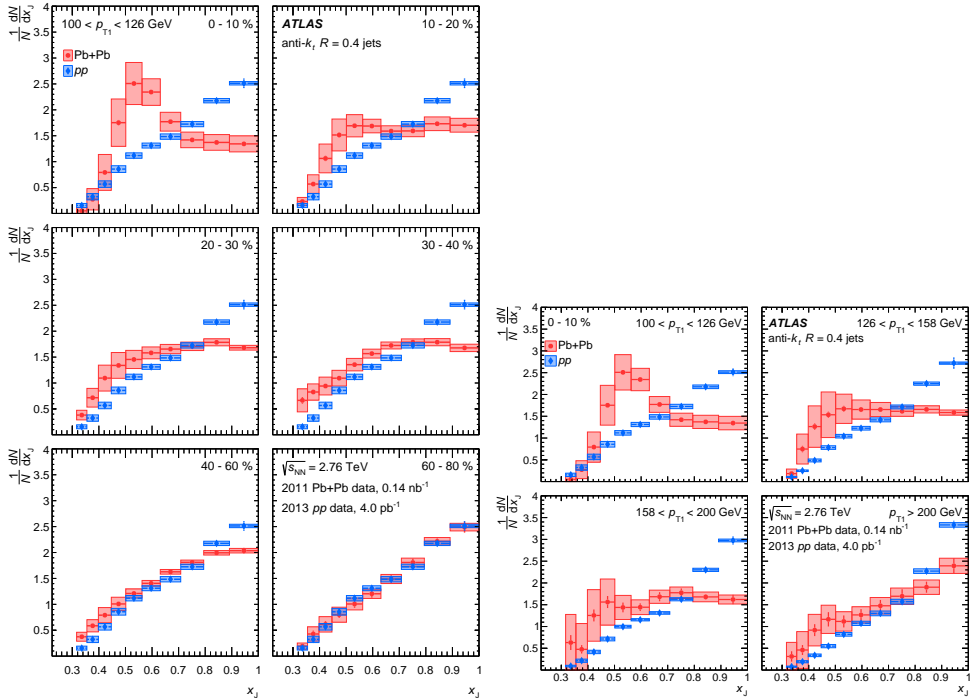


Fig. 4. Left: The $(1/N)dN/dx_J$ distributions for jet pairs with $100 < p_{T1} < 126$ GeV for different collision centralities and for $R=0.4$ jets. The Pb+Pb data are shown in red circles, while the pp distribution is shown for comparison in blue diamonds and is the same in all panels. Right: The $(1/N)dN/dx_J$ distributions with different selections on p_{T1} , shown for the 0–10% centrality interval (red circles) and for pp (blue diamonds). In both panels the statistical uncertainties are indicated by the error bars while systematic uncertainties are shown with shaded boxes¹⁰.

pp collisions and MC. The modification is smaller in the most peripheral centrality interval, 30–50%, and for larger photon momentum, suggesting lower fraction of energy loss with increasing parton p_T .

3. Conclusions

Inclusive jet yields are found to be suppressed with collision centrality, reaching a factor of two in central collisions, while showing little dependence on jet transverse momentum and rapidity. The jet structure in Pb+Pb collisions is modified: in central collisions there is an enhancement of particles at low and high z , while a suppression at intermediate z is observed. The p_T balance of dijets produced in Pb+Pb collisions is increasingly asymmetric when compared to the pp results as the centrality of the collisions increases. At larger values of p_{T1} the x_J distributions are observed to narrow and the differences between the distributions in central Pb+Pb and pp collisions become much smaller. The jet-to-photon transverse momentum ratio, $x_{J\gamma}$, measured in Pb+Pb collisions is observed to be modified with

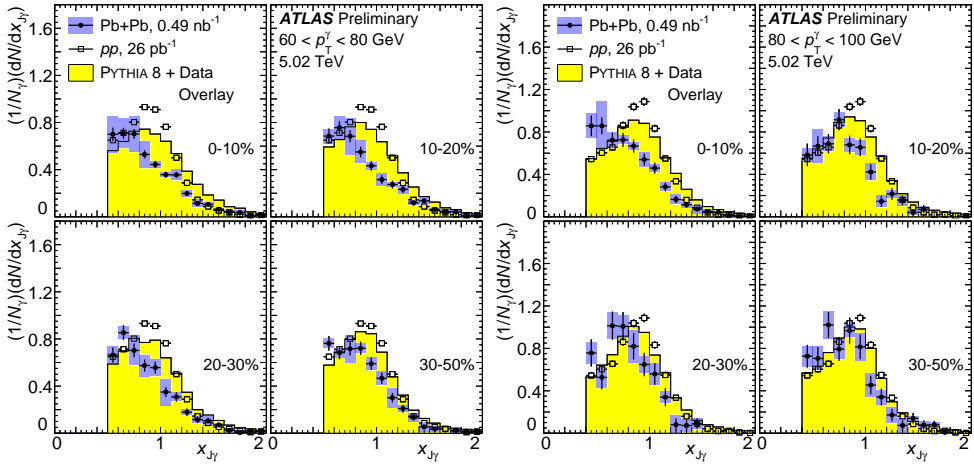


Fig. 5. Measured distributions of the jet-to-photon transverse momentum ratio $x_{J\gamma}$ in $60 < p_{T\gamma} < 80$ GeV (left panel) and $80 < p_{T\gamma} < 100$ GeV (right panel) events, comparing Pb+Pb data (filled circles), pp (open squares), and PYTHIA 8 simulation overlaid with Pb+Pb data (yellow histogram). Each panel shows a different selection on the Pb+Pb event centrality. The vertical bars and the shaded bands show the statistical and systematic uncertainties on the Pb+Pb data, respectively¹¹.

respect to pp collisions and simulation in a way that is systematic in centrality and $p_{T\gamma}$, in a scenario consistent with parton-energy loss in the hot nuclear medium.

Acknowledgments

This work was supported in part by FCT under the contract Project IF/01586/2014/CP1248/CT0003 and Fundação Oriente.

References

1. J.-P. Blaizot and Y. Mehtar-Tani, *J. Mod. Phys.* **E24** (2015) 1530012 (and references therein). arXiv: 1503.05958 [hep-ph].
2. ATLAS Collaboration, *JINST* **3** (2008) S08003.
3. M. L. Miller, K. Reygers, S. J. Sanders, and P. Steinberg, *Ann. Rev. Nucl. Part. Sci.* **57** (2007) 205.
4. ATLAS Collaboration, *ATLAS-CONF-2017-009*. <https://cds.cern.ch/record/2244820>
5. J. W. Cronin et al., *Phys. Rev. D* **11** (1975) 3105.
6. CMS Collaboration, *Phys. Rev. C* **84** (2011) 024906. arXiv: 1102.1957 [nucl-ex].
7. ATLAS Collaboration, *ATLAS-CONF-2017-005*. <https://cds.cern.ch/record/2244802>
8. ATLAS Collaboration, Submitted to PLB. arXiv:1706.02859 [hep-ex].
9. ATLAS Collaboration, *Phys. Rev. Lett.* **105** (2010) 252303. arXiv:1011.6182 [hep-ex].
10. ATLAS Collaboration, *Phys. Lett. B.* **774** (2017) 379. arXiv:1706.09363 [hep-ex].
11. ATLAS Collaboration, *ATLAS-CONF-2016-010*. <https://cds.cern.ch/record/2220772>